BNL-229197-2025-TECH
EIC-ADD-TN-155

Betatron detuning in RHIC and HSR

S. Peggs

December 2025

Electron-Ion Collider

Brookhaven National Laboratory

U.S. Department of Energy

USDOE Office of Science (SC), Nuclear Physics (NP)

DISCLAIMER

Betatron detuning in RHIC and HSR

Angelika Drees, Steve Peggs, Guillaume Robert-Demolaize

December 8, 2025

Contents

1 Nomenclature **2**

2 Octupoles in RHIC and HSR **4**

3 Independent control of κ_{xx} and κ_{xy} **6**

4 Results – theory **7**

5 Results – tracking **8**

6 Acknowledgments **9**

List of Figures

1 Octupoles and their power supplies in RHIC. 5
2 The accessible area in the RHIC $(\kappa_{xx}, \kappa_{xy})$ detuning plane at injection 7
3 Theoretical prediction compared with tracking results in RHIC at injection 8

List of Tables

1 RHIC arc corrector parameters. 3
2 Optical parameters for the RHIC injection lattice Au25-100GeV-qgt24::injection 4
3 HSR detuning coefficient ranges with 137 octupoles 4
4 Extreme values for κ_{xx} and κ_{xy} in RHIC at injection 7

1 Nomenclature

The detuning coefficients κ_{xx}, κ_{xy}, and κ_{yy} are defined in general by the equations

$$\begin{aligned} Q_x(J_x, J_y) &= Q_{x0} + \kappa_{xx} \langle J_x \rangle + \kappa_{xy} \langle J_y \rangle \\ Q_y(J_x, J_y) &= Q_{y0} + \kappa_{xy} \langle J_x \rangle + \kappa_{yy} \langle J_y \rangle \end{aligned} \tag{1}$$

in a linear approximation that is valid when the average horizontal and vertical actions $\langle J_x \rangle$ and $\langle J_y \rangle$ are small. The coefficients have the dimensions of inverse length, since action has the dimension of length. At a location with horizontal Twiss functions β_x, α_x, and γ_x the turn-by-turn physical horizontal phase space co-ordinates are

$$\begin{aligned} x &= \sqrt{2J_x\beta_x} \quad \sin(\phi_x) \\ x' &= \sqrt{2J_x/\beta_x} \quad [\cos(\phi_x) - \alpha_x \sin(\phi_x)] \end{aligned} \tag{2}$$

where the horizontal phase ϕ_x advances by an average of $2\pi Q_x$ each turn. The horizontal action J_x on one particular turn is derived from the physical co-ordinates through the equation

$$2J_x = \beta_x x'^2 + 2\alpha_x x x' + \gamma_x x^2 \tag{3}$$

Normalized phase space co-ordinates x_n and x'_n are related to physical co-ordinates through the Floquet transformation

$$\begin{pmatrix} x_n \\ x'_n \end{pmatrix} = \begin{pmatrix} 1/\sqrt{\beta_x} & 0 \\ \alpha_x/\sqrt{\beta_x} & \sqrt{\beta_x} \end{pmatrix} \begin{pmatrix} x \\ x' \end{pmatrix} \tag{4}$$

which shows that both have the dimensions of root length. The normalized amplitude is therefore

$$a_n \ [\mathrm{m}^{1/2}] = \sqrt{2J} \tag{5}$$

and the physical amplitude is

$$a_p \ [\mathrm{m}] = \sqrt{\beta}\, a_n = \sqrt{2J\beta} \tag{6}$$

either horizontally or vertically.

The values of the detuning coefficients depend on the strengths of nonlinear magnets – primarily sextupoles and octupoles. In octupole-dominated lattices the coefficients can be derived by first order perturbation theory [1]. However, sextupoles are always powered in RHIC and the HSR, in order to control chromaticity. Further, sextupole harmonics must be included in the arc dipoles of RHIC and HSR, if accurate results are required. Second (and higher) order perturbation theory is required to quantify sextupolar detuning. In practice accurate detuning coefficients must be derived from tracking data analysis [2].

The RHIC online model and MAD-X use the same convention to quantify the local octupole strength, namely

$$K3 \ [\mathrm{m}^{-4}] = \frac{1}{(B\rho)} \frac{d^3 B_y}{dx^3} \tag{7}$$

where the vertical field at displacement x is

$$B_y = \frac{1}{6} \frac{d^3 B_y}{dx^3} x^3 \tag{8}$$

Equations 7 and 8 show that

$$\frac{d^3 B_y}{dx^3} \ [\mathrm{Tm}^{-3}] = \frac{6}{(0.025)^3} B_{25} \ [\mathrm{T}] \tag{9}$$

where B_{25} is the vertical field at a displacement of 25 mm. The integrated geometric octupole strength is

$$K3.L \ [\mathrm{m}^{-3}] = \frac{L}{(B\rho)} \frac{d^3 B_y}{dx^3} [\mathrm{m}^{-3}] \tag{10}$$

at a given rigidity, or

$$K3.L \ [\mathrm{m}^{-3}] = 3.84 \times 10^5 \frac{L}{(B\rho)} B_{25} [\mathrm{T}] \tag{11}$$

Table 1 lists the operating parameters of the octupoles and other arc correctors in RHIC [3]. The effective length and B_{25} values listed there yield a bipolar integrated strength range of

$$(K3.L)_{range} \;=\; \pm\frac{3.728\times10^3}{(B\rho)}\;[\mathrm{m}^{-3}] \tag{12}$$

For example, EIC gold rigidities at injection (10 GeV/u) and top storage energy (110 GeV/u) are $(B\rho) =$ 82.8 Tm and 914.8 Tm, respectively, with octupole strength ranges of

$$\begin{aligned} (K3.L)_{range} &= \pm45.02\;[\mathrm{m}^{-3}] \qquad \text{injection} \\ &= \pm\;4.08\;[\mathrm{m}^{-3}] \qquad \text{storage} \end{aligned} \tag{13}$$

Multipole	**Inductance**	**Operating current**	**B-field at 25 mm B_{25}**	**Effective length**	**Quench current**
	mH	A	T	m	A
Decapole	5	59.0	0.016	0.575	202
Octupole	8	50.6	0.017	0.571	198
Quadrupole	29	49.8	0.067	0.555	190
Dipole	840	52.2	0.596	0.508	160

Table 1: RHIC arc corrector parameters [3]. All corrector power supplies are bipolar.

2 Octupoles in RHIC and HSR

A total of 90 octupoles are currently powered in RHIC, 45 apiece at D and F locations, as shown in Figure 1. Their approximate FODO Twiss values are

$$\begin{aligned} (\beta_x, \beta_y) &\approx (10, 50)\ [\mathrm{m}] \qquad \mathrm{D} \\ (\beta_x, \beta_y) &\approx (50, 10)\ [\mathrm{m}] \qquad \mathrm{F} \end{aligned} \tag{14}$$

The 24 F and D power supplies (see Figure 1) that drive them are independent, but for simplicity it is assumed here that all N_D and N_F octupoles at D and F locations have *integrated* strengths of K_D and K_F [m^{-3}]. In that case, and if octupoles dominate, the three detuning coefficients are [1]

$$\begin{aligned} \kappa_{xx} &= \frac{1}{16\pi}\left(N_D \left\langle \beta_x^2 \right\rangle_D .K_D \quad + N_F \left\langle \beta_x^2 \right\rangle_F .K_F\right) \\ \kappa_{xy} &= \frac{-2}{16\pi}\left(N_D \left\langle \beta_x \beta_y \right\rangle_D .K_D + N_F \left\langle \beta_x \beta_y \right\rangle_F .K_F\right) \\ \kappa_{yy} &= \frac{1}{16\pi}\left(N_D \left\langle \beta_y^2 \right\rangle_D .K_D \quad + N_F \left\langle \beta_y^2 \right\rangle_F .K_F\right) \end{aligned} \tag{15}$$

The octupole Twiss averages listed in Table 2 for a RHIC gold injection lattice are reasonably close to the FODO values of 100, 500, and 2500 [m^2] that are predicted by Equation 14.

Parameter	**Units**	**Value**
Horizontal base tune, Q_x		28.2340
Vertical base tune, Q_y		29.2282
Horizontal chromaticity		-5.0
Vertical chromaticity		-5.0
Number of D octupoles, N_D		45
Number of F octupoles, N_F		45
Octupole average $\left\langle \beta_x^2 \right\rangle_D$	m^2	162
$\left\langle \beta_x \beta_y \right\rangle_D$	m^2	538
$\left\langle \beta_y^2 \right\rangle_D$	m^2	2142
$\left\langle \beta_x^2 \right\rangle_F$	m^2	2205
$\left\langle \beta_x \beta_y \right\rangle_F$	m^2	517
$\left\langle \beta_y^2 \right\rangle_F$	m^2	151

Table 2: Optical parameters for the RHIC lattice Au25-100GeV-qgt24::injection that is used for injection calculations in this note. The FODO values predicted by Equation 14 are 100, 500, and 2500 [m^2].

Energy & optics	**Octupole count**	**Detuning coefficient ranges**		
		κ_{xx} $10^3\mathrm{m}^{-1}$	κ_{xy} $10^3\mathrm{m}^{-1}$	κ_{yy} $10^3\mathrm{m}^{-1}$
injection	137	$\pm$179.1	$\pm$207.8	$\pm$287.5
storage	137	$\pm$19.7	$\pm$24.0	$\pm$29.4

Table 3: The HSR injection and storage optics are hi-n-inj-101723-proton.bmad and hi-n/275-10-collision/hsr.bmad, with the layout git#17e7f5e69c010f93d5be9cf027e71bec2495beed. The 3 detuning coefficients are not independent, and so (for example) the peak positive values of κ_{xx} and κ_{xy} can not be reached simultaneously, because of the minus sign in Equation 15.

Table 3 records the extreme ranges of the detuning coefficients in the sample HSR lattice git#17e7f5e69c010f93d5be9cf027e71bec2495beed, under the assumption that all power supplies are turned at full strength, as defined by Equation 13. The octupole count of 137 in the lattice is larger than in RHIC despite the removal of 19 octupoles from IR2 and IR6, because it assumes that all octupoles – both arc *and* triplet – are powered.

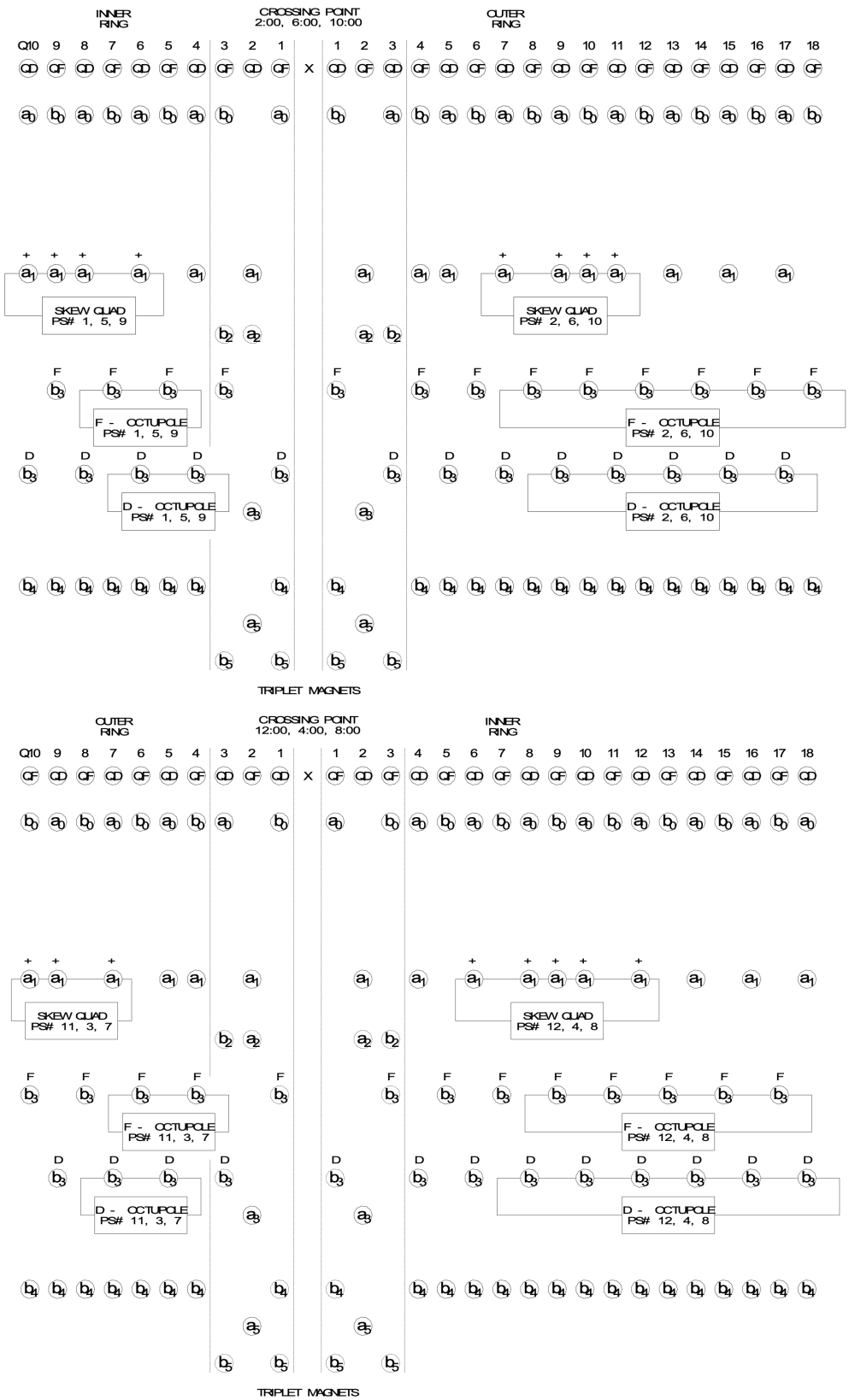

Figure 1: Octupoles and their power supplies in RHIC. Top: IRs 2, 6 and 10. Bottom: IRs 4, 8 and 12. There are also 2 unpowered octupoles – one D and one F – in each of the 12 triplets.

3 Independent control of κ_{xx} and κ_{xy}

Switching to matrix notation Equation 15 is rewritten as

$$\begin{pmatrix} \kappa_{xx} \\ \kappa_{xy} \\ \kappa_{yy} \end{pmatrix} = D_{3\times 2} \begin{pmatrix} K_D \\ K_F \end{pmatrix} + \begin{pmatrix} \kappa_{xx} \\ \kappa_{xy} \\ \kappa_{yy} \end{pmatrix}_{\text{OFFSET}} \tag{16}$$

where the OFFSET vector is usually dominated by sextupoles, and is therefore a nonlinear function of the 2 chromaticities (for a given correction scheme) and the sextupole field components in the arc dipoles. The matrix elements of the 3×2 octupolar detuning matrix $D_{3\times 2}$

$$D_{3\times 2} = \begin{pmatrix} D_{11} & D_{12} \\ D_{21} & D_{22} \\ D_{31} & D_{32} \end{pmatrix} \tag{17}$$

are

$$\begin{aligned} D_{11} &= (N_D/16\pi) \quad \left\langle \beta_x^2 \right\rangle_D \qquad (18) \\ D_{21} &= (-2N_D/16\pi) \left\langle \beta_x \beta_y \right\rangle_D \\ D_{31} &= (N_D/16\pi) \quad \left\langle \beta_y^2 \right\rangle_D \\ D_{12} &= (N_F/16\pi) \quad \left\langle \beta_x^2 \right\rangle_F \qquad (19) \\ D_{22} &= (-2N_F/16\pi) \left\langle \beta_x \beta_y \right\rangle_F \\ D_{32} &= (N_F/16\pi) \quad \left\langle \beta_y^2 \right\rangle_F \end{aligned}$$

Since with 2 free variables (K_D and K_F) only 2 detuning coefficients can be set – say κ_{xx} and κ_{xy} – the situation reduces to a 2×2 matrix equation

$$\begin{pmatrix} \kappa_{xx} \\ \kappa_{xy} \end{pmatrix} = D \begin{pmatrix} K_D \\ K_F \end{pmatrix} + \begin{pmatrix} \kappa_{xx} \\ \kappa_{xy} \end{pmatrix}_{\text{OFFSET}} \tag{20}$$

which is solved for goal detuning values by inverting the D matrix

$$\begin{pmatrix} K_D \\ K_F \end{pmatrix} = D^{-1} \left[\begin{pmatrix} \kappa_{xx} \\ \kappa_{xy} \end{pmatrix}_{\text{GOAL}} - \begin{pmatrix} \kappa_{xx} \\ \kappa_{xy} \end{pmatrix}_{\text{OFFSET}} \right] \tag{21}$$

It's not *prima facie* obvious that sextupoles can be ignored, but it turns out that the OFFSET vector is relatively small in RHIC, even for modest values of K_D and K_F. See Section 5.

4 Results – theory

Figure 2 shows the area in $(\kappa_{xx}, \kappa_{xy})$ space that is predicted to be accessible by two quantitative models:

1. with the simple FODO values of Equation 14, and
2. using the accurate Twiss averages listed in Table 2

Table 4 lists the detuning coefficient values at the four corners of the green parallelogram [4].

D-strength K_D m^{-3}	**F-strength** K_F m^{-3}	**Theory** κ_{xx} m^{-1}	**Theory** κ_{xy} m^{-1}
-45.0	-45.0	-95400	85041
45.0	-45.0	-82341	-1693
-45.0	45.0	82341	1693
45.0	45.0	95400	-85041

Table 4: Detuning coefficient values κ_{xx} and κ_{xy} at the four corners of the green parallelogram shown in Figure 3. These values come from octupole-dominated theory [1], independent of tracking.

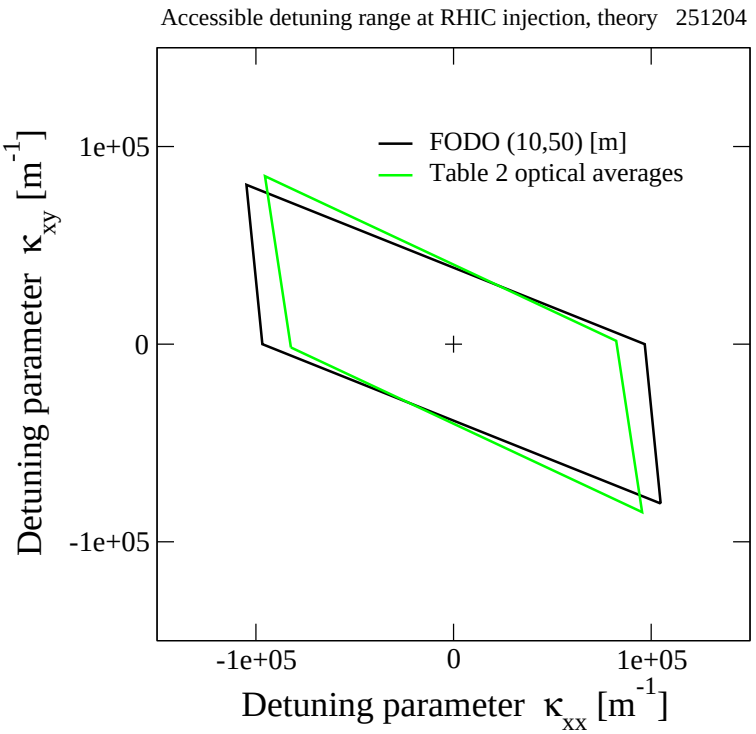

Figure 2: The area in $(\kappa_{xx}, \kappa_{xy})$ space that is theoretically predicted to be accessible in RHIC at injection. The theory does not include sextupolar (OFFSET) terms, which turn out to be negligible. Approximate FODO optics predictions are quite similar to the accurate predictions.

5 Results – tracking

Figure 3 compares theoretical prediction with Sparks [2] tracking results for Q_x versus $\langle J_x \rangle$ with octupoles on (top) and off (bottom). The solid and dashed colored lines are in excellent agreement, showing both that the predictions are accurate (for modest actions), and also that the sextupoles play a negligible role.

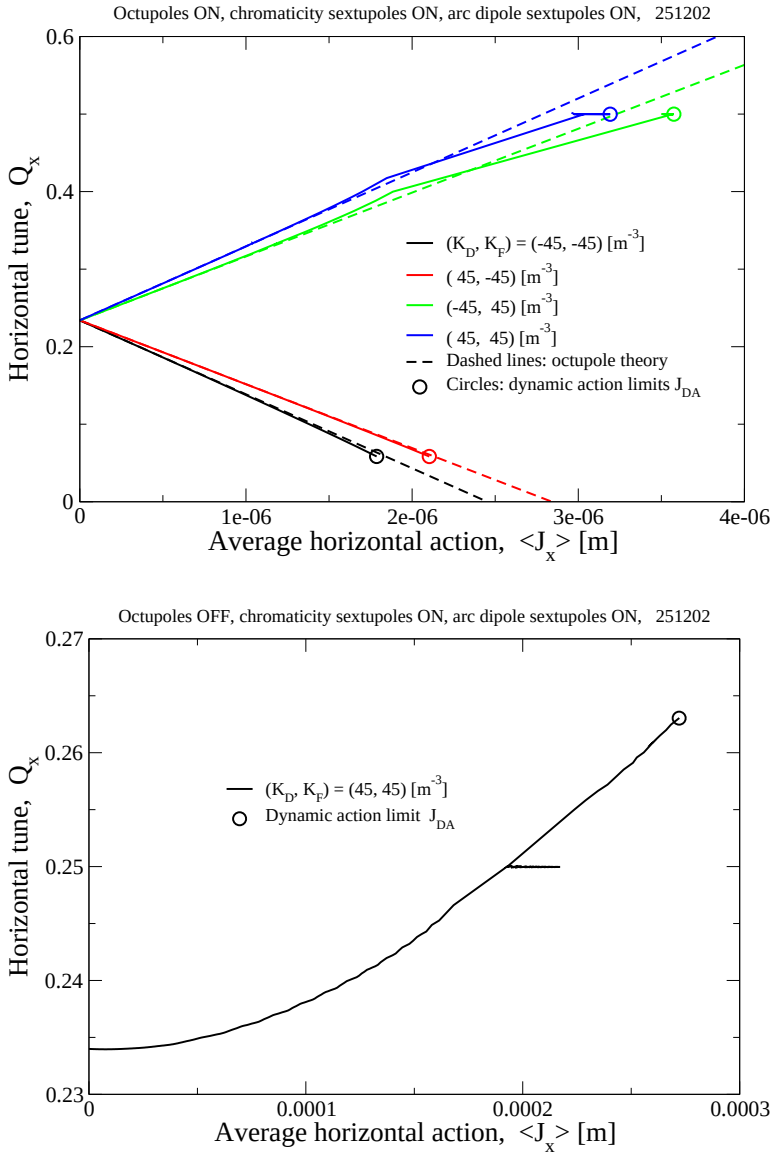

Figure 3: Horizontal tune versus average horizontal action, as measured by the tracking code Sparks [2].
Top: octupoles ON with strengths corresponding to the four corners of the green parallelogram in Figure 2, with stability up to a dynamic action of about $J_{DA} \approx 2.5$ microns.
Bottom: octupoles OFF, still with chromatic sextupoles and arc dipole sextupole components turned on, with a dynamic action about 2 orders of magnitude larger, with $J_{DA} \approx 270$ microns.

The vertical and horizontal scales of the top and bottom plots in Figure 3 are very different. Purely horizontal motion (with no longitudinal motion or $\Delta p/p$ offset) is stable up to a dynamic action J_{DA} of only about 2.5 microns when the octupoles are on at full strength. The dynamic action increases to about 270 microns when the octupoles are turned off, leaving only the chromatic sextupoles turned on, as well as the contributions from sextupole harmonics in arc dipoles. Turning octupoles on at full strength reduces this

crude measure of dynamic aperture by about 2 orders of magnitude.

The natural action scale is the unnormalized RMS emittance ϵ_u, since by definition

$$\epsilon_u \equiv \langle J \rangle_\rho \tag{22}$$

where the average $\langle\rangle_\rho$ is taken over the beam distribution $\rho(J)$. For example, if the normalized RMS emittance is

$$\epsilon_n = 2 \times 10^{-6} \quad [\text{m}] \tag{23}$$

at an injection Lorentz gamma of

$$\gamma = 10.52 \tag{24}$$

then the unnormalized emittance is

$$\epsilon_u = \frac{\epsilon_n}{\gamma} \approx 0.19 \times 10^{-6} \quad [\text{m}] \tag{25}$$

With a modest detuning value of about 10% of the accessible range

$$\kappa_{xx} = 1 \times 10^4 \quad [\text{m}] \tag{26}$$

a typical 1σ particle has a horizontal tune shift of about

$$\Delta Q_x = \kappa_{xx} \epsilon_u \approx 0.002 \tag{27}$$

and an $N\sigma$ particle has

$$\Delta Q_x \approx 0.002 \times N^2 \tag{28}$$

which easily becomes significantly large.

6 Acknowledgments

Many thanks go to Mike Blaskiewicz, Brendan Lepore, Henry Lovelace III, and Vincent Schoefer, for their insightful discussions and for their support in the control room.

References

[1] S. Peggs, H. Lovelace III, G. Robert-Demolaize, and T. Satogata. Resonance Island Jump theory for the HSR. Technical Report EIC-ADD-TN-77, BNL, 2023.

[2] G. Robert-Demolaize. The Sparks tracking code. Technical Report to be published, BNL, 2026.

[3] RHIC Configuration Manual, Table 7-3, p59, 2006.

[4] S. Peggs. See unpublished script `code_python/detuning/points.py`.